

Lecture 9 Cosmic Rays and Magnetic Fields

A. Cosmic Rays

1. Introduction and history
2. Local properties
3. Interactions
4. Ionization rate

B. Magnetic Fields

1. Synchrotron radiation
2. Faraday rotation
3. Zeeman effect
4. Summary

References

- K. Ferrier, Rev Mod Phys, 73, 1031, 2001 (Sec. IV)
- MS Longair, High Energy Astrophysics (Vol. I Ch. 9)
- Zweibel & Heiles, Nature 385 101 1997
- Crutcher, Heiles & Troland, Springer Lecture Notes in Physics, 614 155 2003
- R. Beck, Space Science Reviews, 99, 243, 2001

A. COSMIC RAYS

1. Introduction

DISCOVERY

Part of the rise of “modern” physics: early radiation detectors (ionization chambers, electroscopes) showed a ***dark current*** in the absence of sources.

Rutherford (1903): most comes from radioactivity

Wulf (1910): dark current down by 2 at top of Eiffel Tower -
could not be gamma rays

Hess (1912): 5 km open-balloon flight showed an *increase*

Hess & Kockhörster (by 1914): balloon flights to 9 km ...

Studies of the variation with height, latitude & longitude confirmed the particle nature of ***cosmic rays*** (Millikan's name) originating above the Earth's atmosphere.

Role in Physics and Astrophysics

Anderson discovered the positron in 1932 and shared the Nobel Prize with Hess in 1935.

Until 1952, cosmic ray research was experimental particle physics. It led to many discoveries: muon, pion, and other particles. Even today the energy of the highest energy cosmic rays, $> 10^{20}$ eV, is much higher than is available with accelerators.

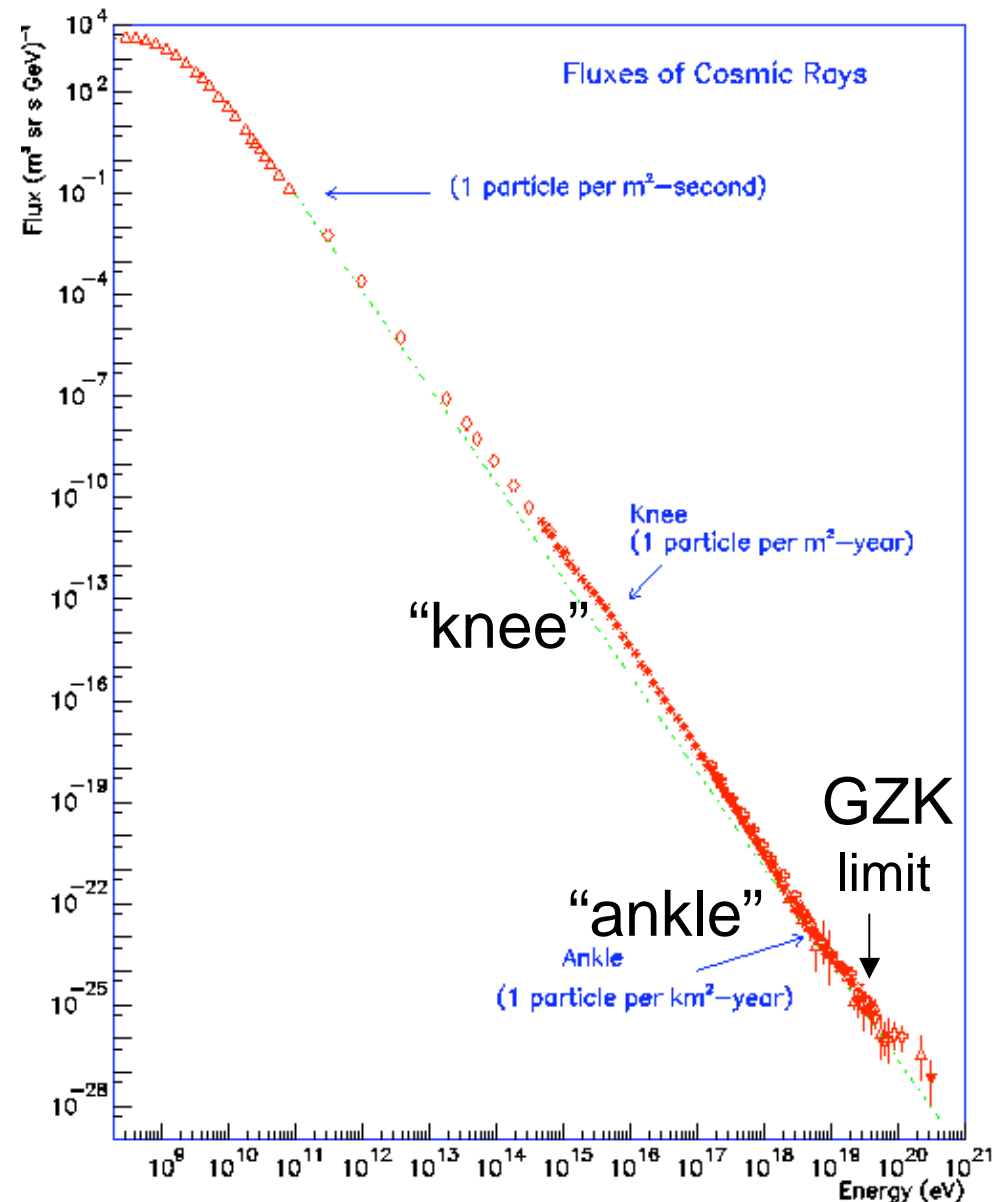
The extraterrestrial nature of cosmic rays might challenged early astronomers, but this did not happen until mid 20th century. Cosmic rays now play an important role in solar system and galactic astrophysics, including the ISM.

Cosmic Ray Spectrum from 10^8 - 10^{21} eV

Power law defined from 10^{10} - 10^{15} eV steepens at the “knee” and recovers beyond the “ankle”.

The ultra high-energy CRs have been a puzzle arose because they can't be confined by galactic B-fields, they can't be produced by SNe, and they can't come from very large distances since they interact with CMB photons.

A solution may be in sight from the Pierre Auger Observatory (Science 318, 938, 2007): Ultra high-energy CRs are anisotropic and appear to be associated with nearby AGN.



2. Locally Properties of Cosmic Rays

From observations above the atmosphere using balloons, rockets and satellites we know (e.g. Longair Vol. I Ch. 9):

1. high degree of isotropy (except for the UHE CRs)
2. power law spectra from 10^9 - 10^{14} eV (and higher)
3. low-energy CRs excluded from solar system
4. (mainly) solar abundances
5. short lifetime in the Milky Way (20 Myr) – c.f. detection of radioactive ^{10}Be (half-life 1.5 Myr) produced by “spallation” reactions with light nuclei
6. significant pressure: $\sim 10^{-12}$ dynes cm^{-2}

Cosmic Ray Spectra

Simpson, ARNS 33 330 1983

Intensity vs. energy per nucleon
from $10 - 10^7$ MeV/A.

The units of intensity are:
particles per ($\text{m}^2 \text{ s MeV/nucleon}$).
The proton slope is -2.75.

$$I_p(E) = 1.67 \times 10^{-3} \left(\frac{E}{\text{GeV}} \right)^{-2.75}$$

$$\text{cm}^{-2} \text{ s}^{-1} \text{ sr}^{-1} \text{ GeV}^{-1}$$

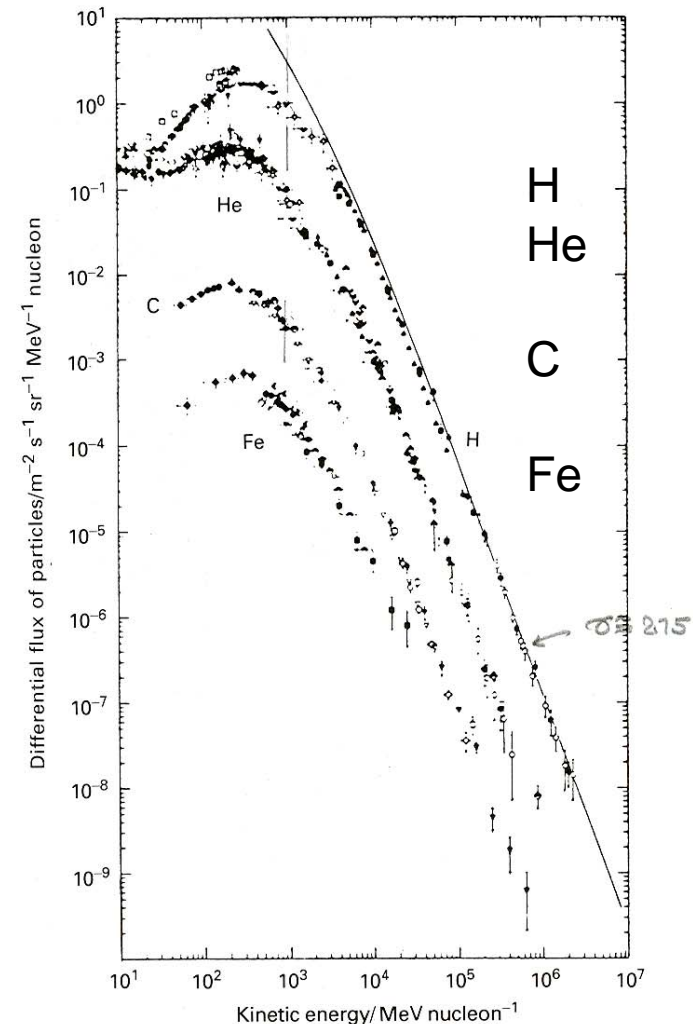
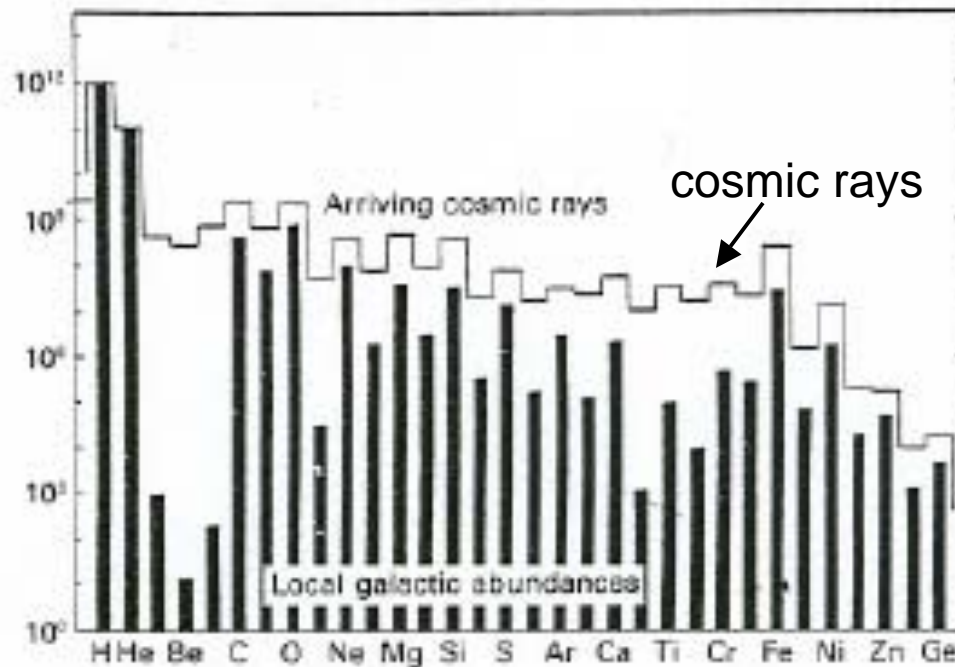


Figure 9.1. The differential energy spectra of cosmic rays as measured from observations made from above the Earth's atmosphere. The spectra of helium, carbon and iron are shown. The solid line shows the unmodulated hydrogen, i.e. the effects of propagation through the interplanetary medium have been eliminated using a model for the process. The flux of helium nuclei below about 60 MeV nucleon⁻¹ is due to the flux of these particles which is known as the anomalous ⁴He component (Simpson (1983). *Ann. Rev. Nucl. Part. Sci.*, **33**, 330).

Cosmic Ray Abundances



The excesses are largely due to ***spallation reactions*** of protons with abundant nuclei that products that ordinarily are produced at low abundances by stellar nucleosynthesis.

3. Interaction of Cosmic Rays with Matter

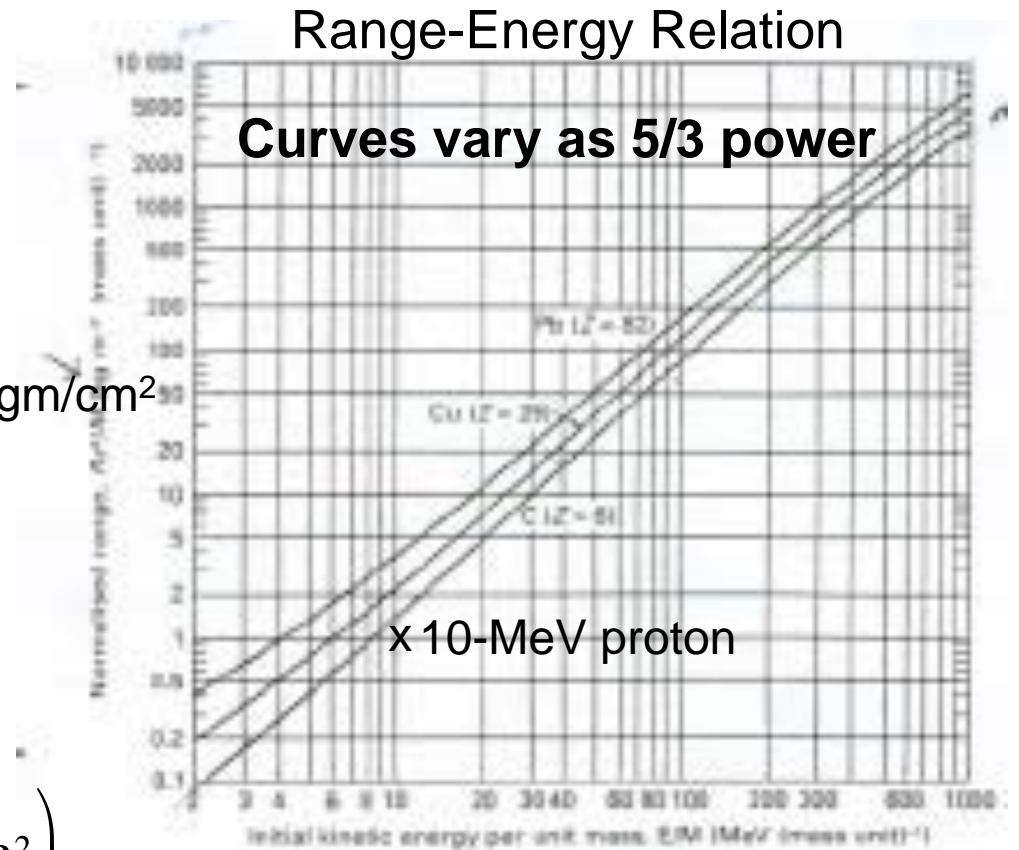
Most CRs have $E \sim 1$ GeV. They interact primarily with atomic electrons, exciting & ionizing atoms. The cross sections are well known from experiment and Bethe's theory.

$$\sigma_{\text{ion}}^{(\text{Bethe})} = 1.23 \times 10^{-20} \text{ cm}^2$$

$$\times (Z/\beta)^2 \left(6.20 + \log \left(\frac{\beta^2}{1 - \beta^2} \right) - 0.43\beta^2 \right)$$

with $\beta = v/c$

R (gm/cm²)




Nuclear and Magnetic Interactions

At GeV energies, the nuclear cross section is ~ 10 mb, equivalent to ~ 100 gr cm⁻²; thus nuclear interactions are less important than electronic.

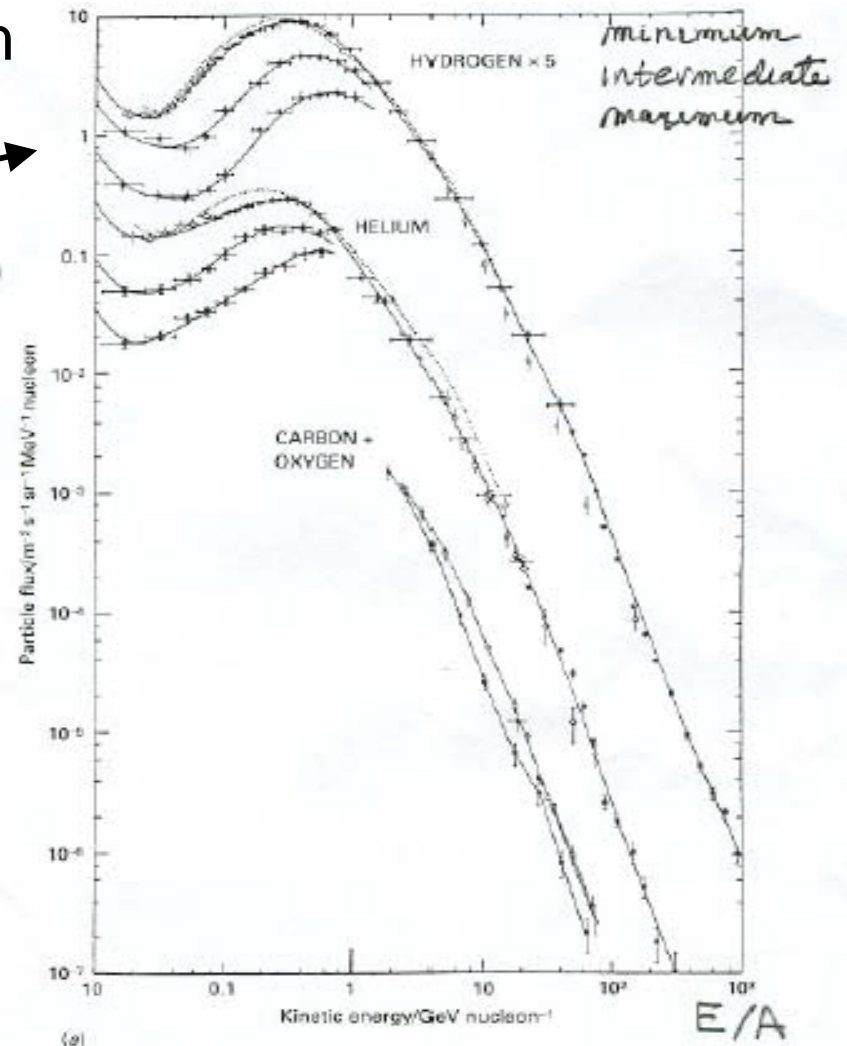
Scattering from bent or kinked magnetic field lines can also be important. It arises from the inability of a charged particle to continue smoothly spiraling around a magnetic field when the fields vary rapidly in space. CRs can also excite Alfvén waves via this magnetic interaction and then interact with these waves. These magnetic processes are especially important where the interstellar turbulence is MHD in nature, and they affect the transport of CRs through the galaxy.

Demodulation of the Low-energy Spectrum

With $I(E)$ decreasing rapidly with E , it is important to understand the low-energy behavior. 

The figure shows spectra at three levels of solar activity, indicating that the Sun itself changes the CR intensity: **the solar wind blows the low-energy galactic CRS away.**

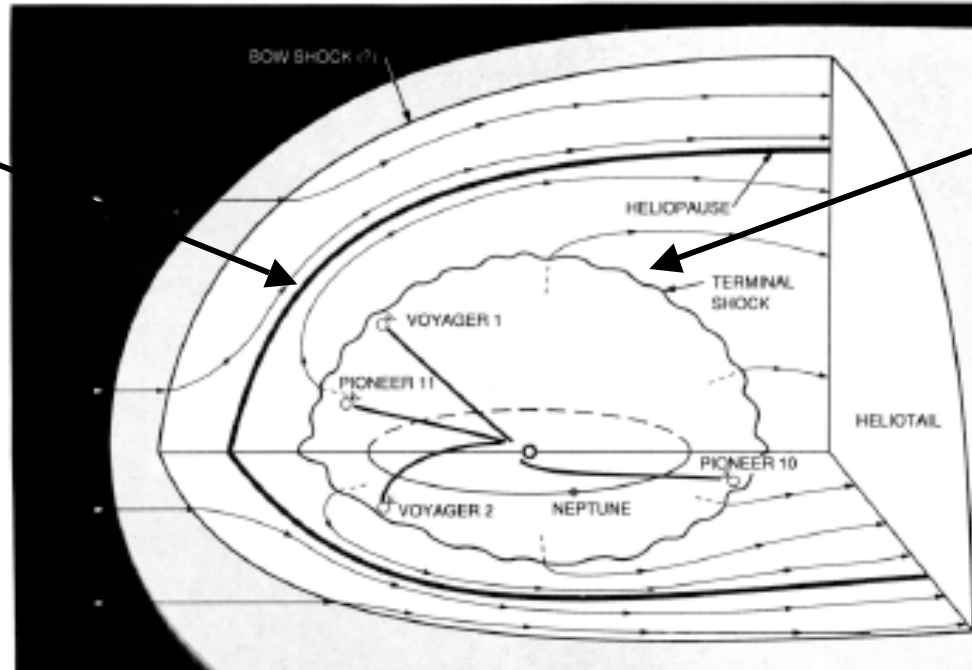
Correcting the observed spectra for such solar system effects, or **demodulation**, is required to deduce the CR intensity in the local ISM.



Longair Vol.1, Fig 10.3a

Shocks in the Heliosphere

Bow shock c.f.
interstellar “wind”
 $v = 23 \text{ km/s}$

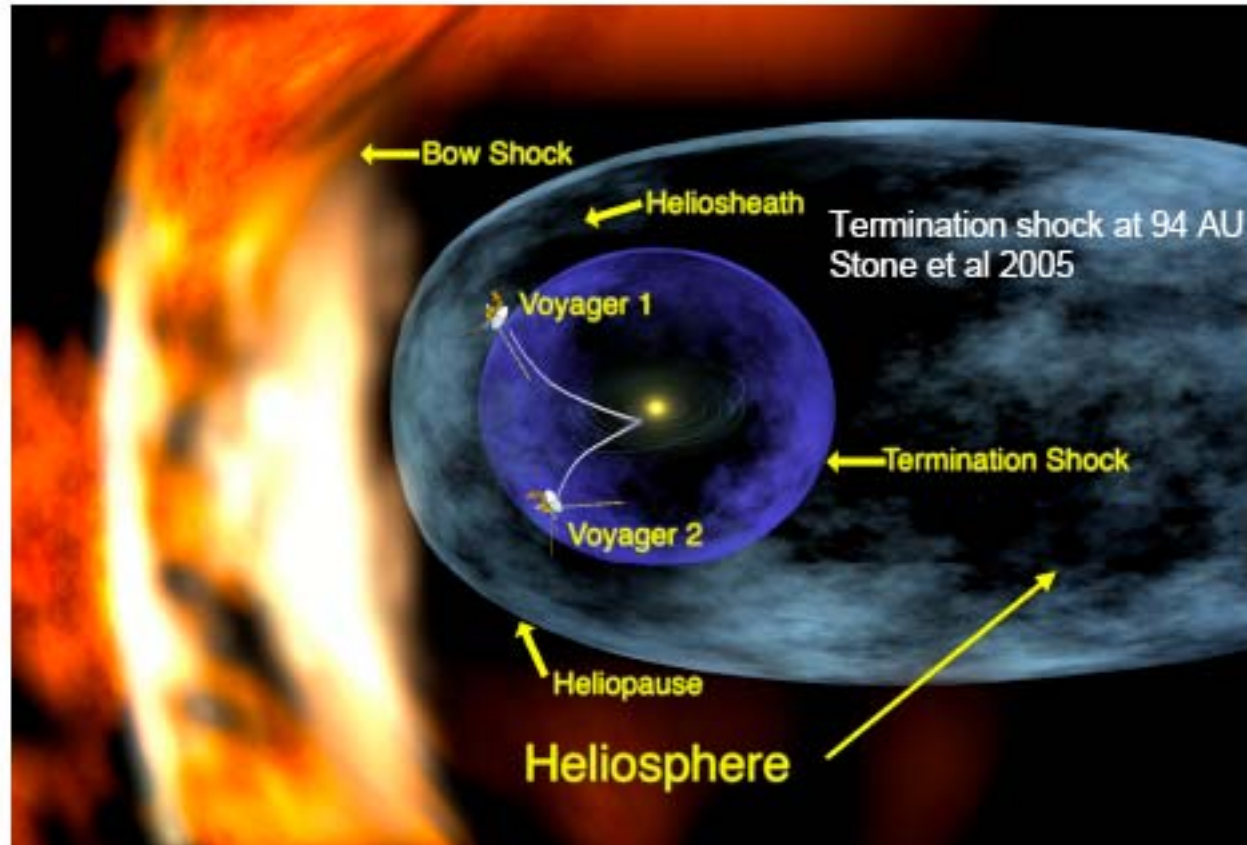


Terminal shock
c.f. solar wind,
 $v \sim 400 \text{ km/s}$

Suess, Rev Geophys 28 1 1990

Demodulating the measured CR intensity applies transport theory to satellite observations as a function of heliocentric distance. The satellites are now in the neighborhood of the crucial terminal shock.

Voyager 2 Crosses the Heliosheath



Voyager 1 and 2 were launched in 1977. Voyager 1 at 105 AU and Voyager 2 at 85 AU are still measuring energetic particles in the neighborhood of the heliosheath, e.g., <http://voyager.jpl.nasa.gov>

4. Cosmic Ray Ionization Rate

Given a demodulated CR intensity, the ionization rate can be calculated by integration with the ionization cross section. H, He, and H₂ are the most important targets. A basic fact is that ~ 37 eV is needed to make an ion pair, so a 2 MeV proton makes about 54,000 ions. The CR ionization rate per proton can be expressed as

$$\zeta_{\text{CR}} = f_{\text{heavy}} f_{\text{sec}} \zeta_{\text{p}}, \quad f_{\text{sec}} \cong \frac{5}{3} \quad f_{\text{heavy}} \cong 2$$

where ζ_{p} is the primary rate at which hydrogen is ionized. Integrating down to 2 MeV (following Spitzer & Tomasko, ApJ 152 971 1969):

$$\zeta_{\text{p}} \approx 6 \times 10^{-18} \text{ s}^{-1} \text{ and } \zeta_{\text{CR}} \approx 2 \times 10^{-17} \text{ s}^{-1}$$

With a more recent demodulation model, the rate becomes

$$\zeta_{\text{CR}} \approx 5 \times 10^{-17} \text{ s}^{-1}$$

or possibly somewhat higher (Webber, ApJ 506 334 1998)

B. Interstellar Magnetic Field

Early History

- Started in 1949 with the discovery of the polarization of starlight by interstellar dust (Hall & Hiltner).
- Explained in terms of paramagnetic grains spinning about their short axes aligned with the magnetic field (Davis & Greenstein 1951).
- Shklovsky (1953) suggested that synchrotron radiation powers the Crab Nebula; optical polarization was found the next year by Russian astronomers.
- Searches for the Zeeman splitting of the 21-cm line were proposed by Bolton & Wild in 1957.

1. Optional Review of Synchrotron Radiation

References

Jackson Ch. 14

Rybicki & Lightman Ch. 6

Shu I Ch. 18

Charged particles undergo helical motion around magnetic field lines. A key parameter is the **cyclotron frequency** ω_B . The relativistic mechanics of a particle with charge q and rest mass m_0 in a uniform field \mathbf{B} can be stated as:

$$\frac{d\vec{v}}{dt} = \vec{\omega}_B \times \vec{v} \quad \vec{\omega}_B = \frac{1}{\gamma} \left(\frac{q\vec{B}}{m_0 c} \right)$$

$$\gamma = \frac{1}{\sqrt{1 - \beta^2}} \quad \beta = v/c$$

$$\nu_B(\text{e}) = 2.80 \text{ Hz} \frac{1}{\gamma} \left(\frac{B}{\mu\text{G}} \right)$$

Rotating Vector Solution

The motion is decomposed into a ***drift motion*** along the field and a ***circular motion*** perpendicular to the field:

$$\vec{v} = \vec{v}_{\parallel} + \vec{v}_{\perp}.$$

In the absence of other forces, the drift motion is free and the circular motion is described by the *rotating vector*:

$$\vec{r} = a (\cos \varpi_B t \hat{x} + \sin \varpi_B t \hat{y}) = \text{Re } a e^{-i\varpi_B t} (\hat{x} + i\hat{y})$$

$$\vec{v} = \varpi_B a (-\sin \varpi_B t \hat{x} + \cos \varpi_B t \hat{y}) = \text{Re}(-i\varpi_B \vec{r})$$

$$\dot{\vec{v}} = -\varpi_B^2 \vec{r}.$$

One also derives expression for for the gyroradius,

$$a = \frac{cp_{\perp}}{|q|B} = \frac{p_{\perp}}{m_0\omega_B} = \left(\frac{c}{\omega_B} \right) \left(\frac{v_{\perp}}{c} \right)$$

Orbital Properties of Charged Particles

The numerical value of the cyclotron frequency ($\gamma=1$) are:

$$\omega_B = 17.59 \text{ MHz } B \text{ for electrons}$$

$$\omega_B = 9.590 \text{ kHz } B (Z/A) \text{ for ions}$$

For a typical interstellar magnetic field of $5 \mu\text{G}$, the orbital period and radii are:

particle	$2\pi/\omega_B$ (in s)	c/ω_B (in cm)
electron	0.0714	3.4×10^8
proton	131	6.26×10^{11}

Small by interstellar standards, these numbers validate the spiraling motion of electrons and ion along interstellar magnetic field lines,

Standard Treatment of Synchrotron Radiation

Basis

- circular orbits, gyrofrequency ω_B
- Lorentz factor γ
- helical pitch angle α
- L-W retarded potentials
- relativistic limit $\gamma \gg 1$

Results

1. Mean Power

$$\frac{dP(\varpi)}{d\varpi} = \frac{2}{3} \frac{q^2}{c} (\varpi_B \beta \sin \alpha)^2 \gamma^4$$

(relativistic Larmor formula)

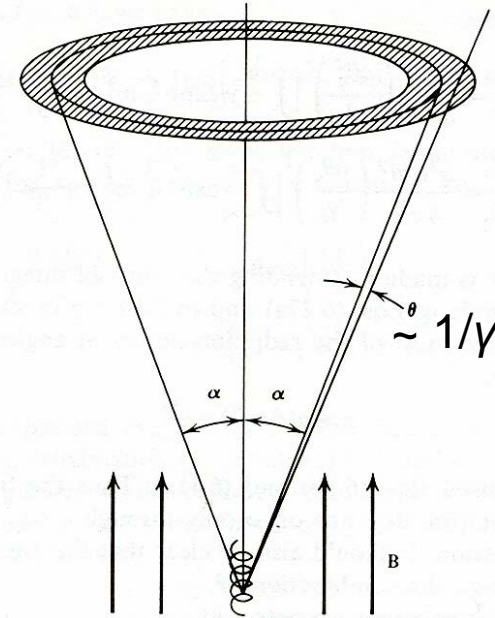


Figure 6.5 Synchrotron emission from a particle with pitch angle α . Radiation is confined to the shaded solid angle.

Rybicki-Lightman Fig. 6.5b

Synchrotron Radiation Results

2. **Angular Distribution** – searchlight in cone of half-angle α about \mathbf{B} and width $1/\gamma$ (previous figure).

3. **Frequency Distribution** -

$$\frac{dP(\omega)}{d\omega} = CF\left(\frac{\omega}{\omega_c}\right)$$

$$\omega_c = \frac{2}{3} \gamma^3 \omega_B \sin \alpha$$

$$C = \frac{\sqrt{3}}{2\pi} \left(\frac{q^2}{c^2}\right) \left(\frac{|q|B}{m_0 c}\right) \sin \alpha$$

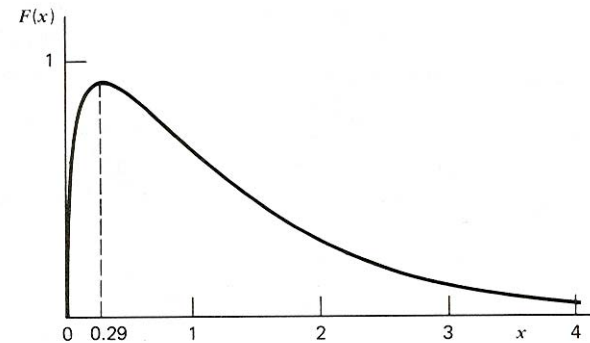


Figure 6.6 Function describing the total power spectrum of synchrotron emission. Here $x = \omega/\omega_c$. (Taken from Ginzburg, V. and Syrovatskii, S. 1965, *Ann. Rev. Astron. Astrophys.*, 3, 297.)

F plotted vs. ω/ω_c
(Rybicki & Lightman Fig. 6.6)

4. **Polarization** ~ 75%, integrated over the spectrum for fixed γ , the emission is **plane-polarized** in the plane of the sky (perpendicular to the line of sight), the classic signature of synchrotron emission.

Synchrotron Radiation Results

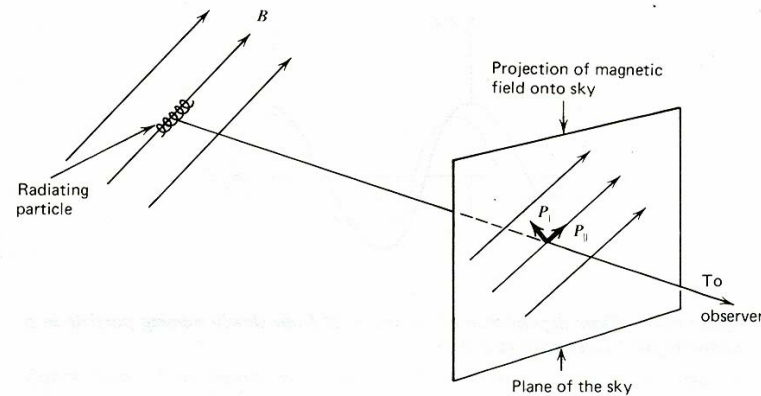


Figure 6.7 Decomposition of synchrotron polarization vectors on the plane of the sky.

The radiation from an ultra-relativistic particle is mainly polarized in the plane of motion, i.e., perpendicular to \mathbf{B} (Jackson, Sec. 14.6)

5. Power Law Electron Energy Distribution – suggested by the local cosmic ray spectrum and the observed spectrum

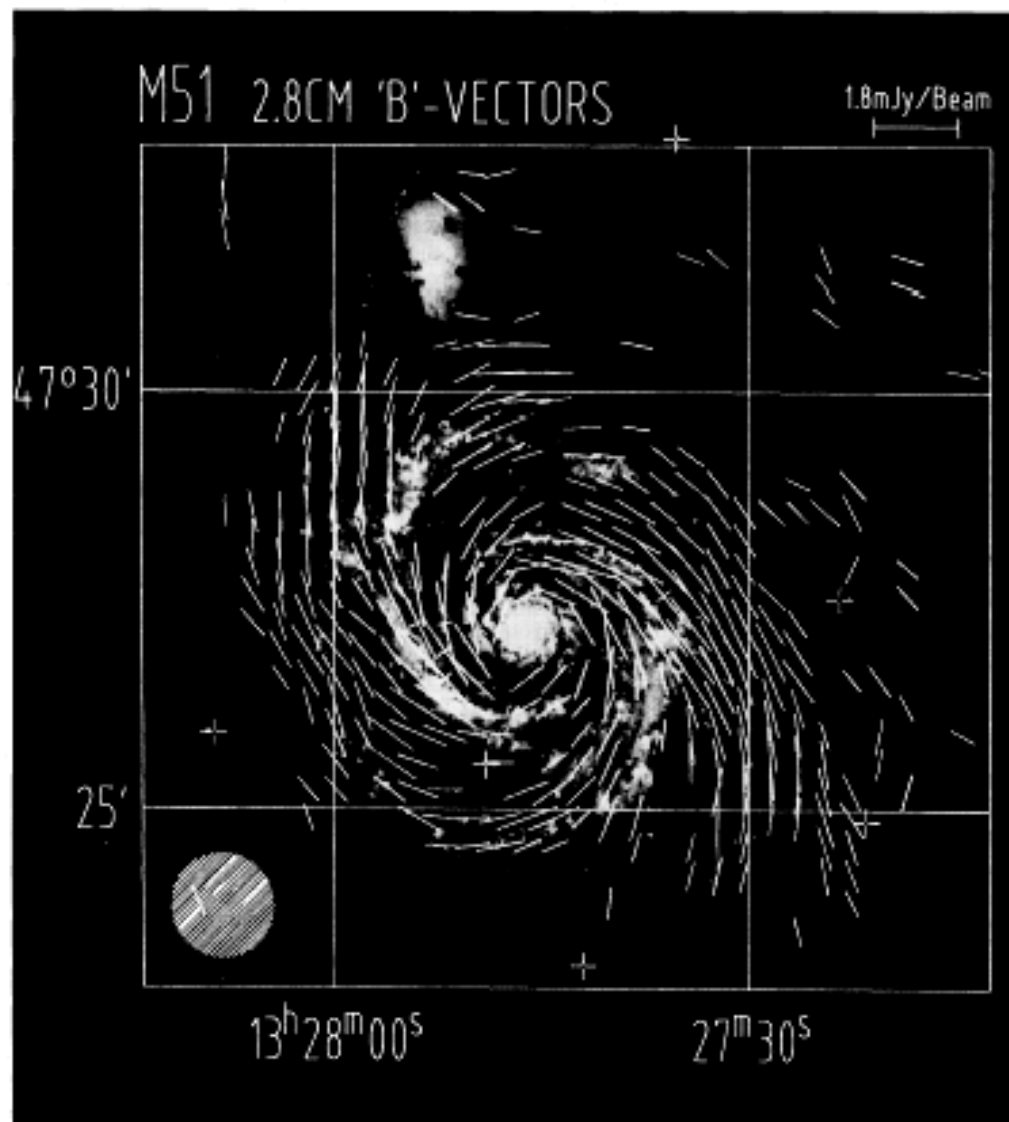
$$\frac{dN(\gamma)}{d\gamma} = D \gamma^{-p} \Rightarrow \frac{dP(\omega)}{d\omega} \propto \left(\frac{B \sin \alpha}{\omega} \right)^{\left(\frac{p-1}{2} \right)}$$

The observations suggest $p \sim 3$.

Results of Synchrotron Observations

- The main characteristics of synchrotron radiation, ***polarization and power-law spectra***, are observed towards extragalactic radio sources (and pulsars).
- They tracing the field direction in external galaxies, as illustrated for M51 and NGC 891 (figures below).
- The magnitude of the field cannot be determined without making assumptions about the electron density, since the flux is proportional to $B^2 n_e$. The usual assumptions are (1) cosmic ray electron and proton pressures are proportional to one another and (2) the particle and magnetic pressures are roughly equal.
- For the Milky Way, the results in the solar neighborhood are:

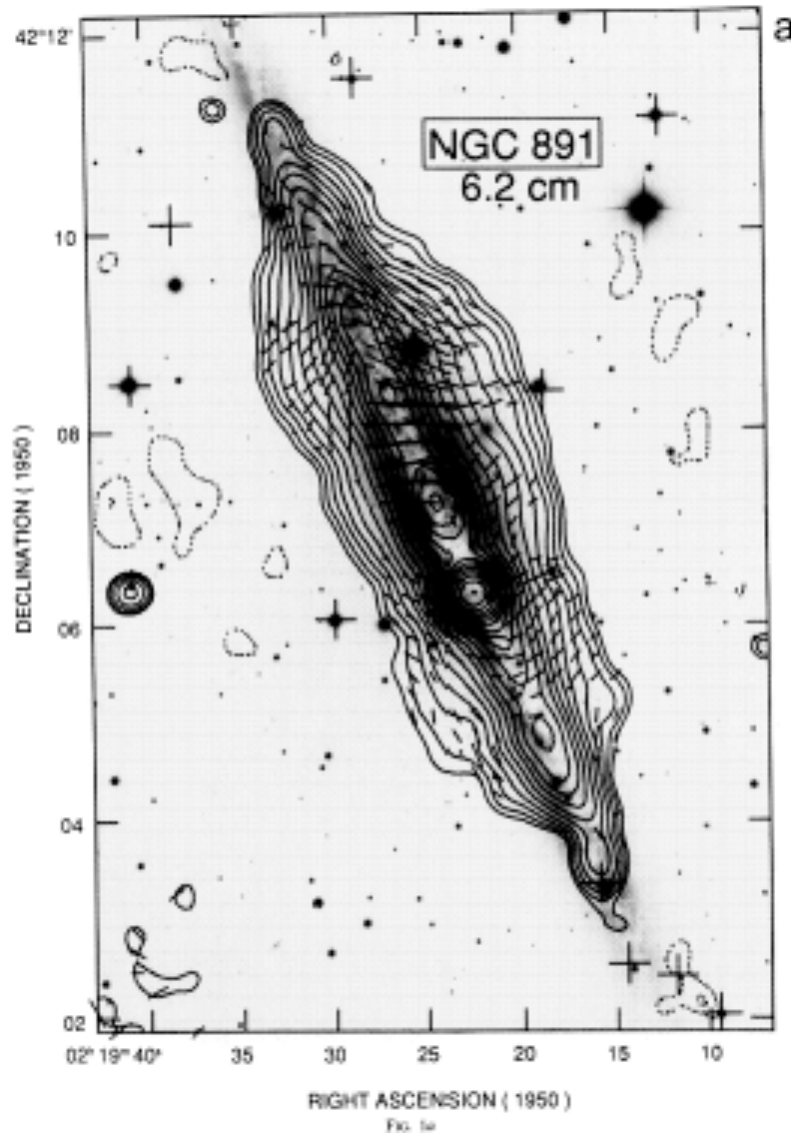
$$\begin{aligned} B &\sim 5 \mu\text{G} \\ H_z &\sim 4.5 \text{ kpc} & H_R &\sim 12 \text{ kpc} \end{aligned}$$



2.8 cm observations of polarized emission from the face-on galaxy M51. ***The magnetic field directions follow the spiral arms.***

Fig. 3. *B*-vectors of the intrinsic magnetic field of M51, obtained by rotating the measured *E*-vectors by 90° superimposed onto the same optical plate as Fig. 2. The length of the vectors is proportional to the polarized intensity

Neininger, A&A 263 30 1993



6 cm synchrotron emission
from the edge-on galaxy
NGC 891 showing
halo emission.

Sukumer & Allen
ApJ 382 100 1991

***Magnetic fields as well as
cosmic rays must extend
above the disk of the
galaxy.***

3. Faraday Rotation

In 1845 Faraday discovered that the polarization of an EM wave can change in a magnetic field. Measuring the degree of polarization along the line of sight toward pulsars provides important information on the interstellar magnetic field, especially the WIM.

Generalizing Lec07, the **index of refraction of a magnetized plasma** is obtained by combining Maxwell's equations (for harmonic variations) with Newton's equation for an electron, including the Lorentz force (e.g., Shu Vol. I, Ch. 20)

$$n_{\pm}^2 = 1 - \frac{\omega_{pl}^2}{\omega(\omega \mp \omega_B)}$$

$$\omega_{pl} = \sqrt{\frac{4\pi n_e e^2}{m_e}} = 5.63 \times 10^4 \sqrt{n_e} \text{ Hz}, \quad \omega_B(e) = 17.6 \left(\frac{B}{\mu G} \right) \text{ Hz}$$

Assume that circularly polarized radiation travels in the direction of the field (z):

$$\vec{E} = \vec{E}_0 (\hat{x} \pm i\hat{y}) e^{i(k_{\pm} z - \omega t)} \quad k_{\pm} = n_{\pm} (\omega / c)$$

Circularly Polarized Radiation

After it travels a distance z , it can be represented as

$$\vec{E}(z, t) = (\vec{E}_0 / 2) \left((\hat{x} + i\hat{y})e^{i(k_+ z - \omega t)} + (\hat{x} - i\hat{y})e^{i(k_- z - \omega t)} \right)$$

with the right and left amplitudes propagating with different phases. After a little algebra, this becomes

$$\vec{E} = \vec{E}_0 e^{i(Kz - \omega t)} (\hat{x} \cos \psi + \hat{y} \sin \psi)$$

$$\psi = \frac{1}{2}(k_+ - k_-)z = \frac{1}{2}(n_+ - n_-)\frac{\omega}{c}z \quad K = \frac{1}{2}(k_+ + k_-)$$

where ψ is the rotation of the plane of polarization. It involves the difference in the index of refraction:

$$\Delta n = \frac{1}{2} \frac{\omega_{pl}^2}{\omega^2} \frac{\omega_B}{\omega} \Rightarrow \boxed{\psi = \frac{\omega_{pl}^2}{\omega^2} \frac{eB}{2m_e c^2} z}$$

Rotation Measure RM

Integrating along the line of sight, the net rotation of the plane of polarization is expressed in terms of the

Faraday Rotation Measure:

$$\psi = 2\pi \frac{e^3}{m_e c^4} \lambda^2 RM, \quad RM \equiv \int ds n_e B_{\parallel} \approx L_{\parallel} \langle n_e \rangle \langle B_{\parallel} \rangle$$

Since we cannot measure absolute phases (not knowing the polarization of the source), the wavelength dependence of the RM is measured, assuming that the initial polarization is independent of wavelength.

RM s are measured towards pulsars and extragalactic radio sources (see the following figures). For pulsars, measurements of the RM and DM yield values of B_{\parallel} that are somewhat smaller than the synchrotron result for the WIM ($\sim 5 \mu\text{G}$), presumably due to ignoring the correlation between n_e and \mathbf{B} .

Pulsar *RM* Measurements

8

RAINER BECK

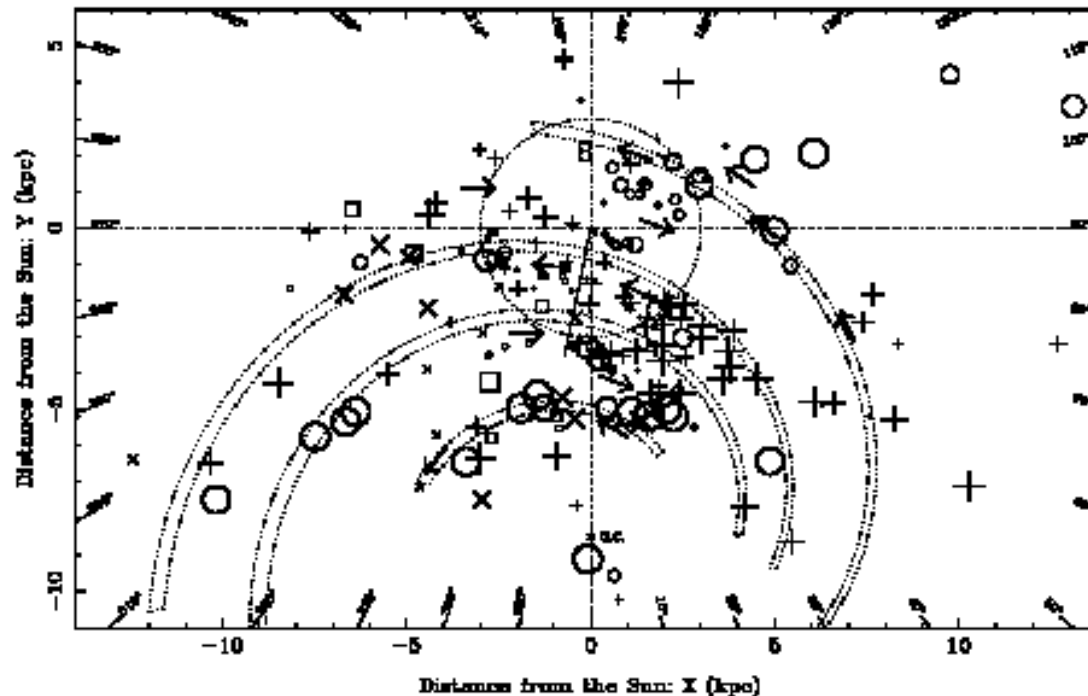


Figure 2. The distribution of the *RM*s of pulsars within 8° of the Galactic plane. Positive *RM*s are shown as crosses, negative *RM*s as circles. The most recent *RM* data are indicated by X and open squares. The symbol sizes are proportional to the square root of $|RM|$, with the limits of 5 and 250 rad/m². The directions of the bisymmetric field model are given as arrows. The approximate location of four spiral arms is indicated as dotted lines. The dotted circle has a radius of 3 kpc (from Han *et al.*, 1999a).

Pulsar *RM*s within 8° of the galactic plane.
positive values + negative values o

R. Beck, SSR 99 243 2001

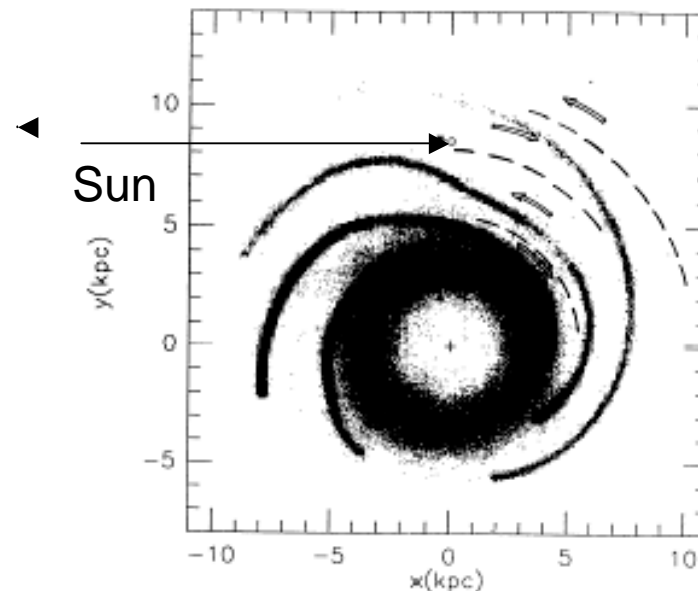
Field Reversals

The field reversals are believed to occur in between the spiral arms. The early results of Rand & Lyne (1994) are superimposed on the electron density model of Taylor & Cordes (1993) discussed in Lec08

514

C. HEILES

Heiles, ASP 80 497 1995



Arrows: field directions
Dashed lines: reversals

Figure 1. The magnetic field directions (double arrows) and reversals (dashed lines; Rand and Lyne 1994), and $\langle n_e \rangle$ ("grey scale"; Taylor and Cordes 1993). The reversals are shown as sectors of circles; in the text, we surmise that the reversals may be spirals and lie in interarm regions.

Extragalactic RM s

Extragalactic RM s:
closed circles > 0
open circles < 0

R Beck SSR 99 243 2001

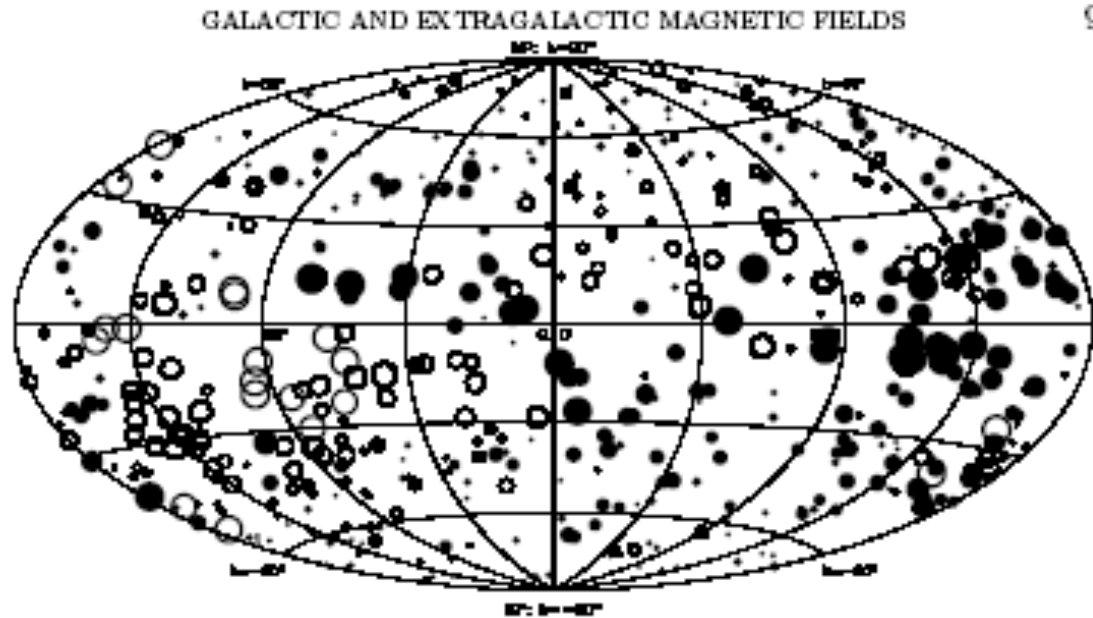


Figure 3. The distribution of the RM s of extragalactic radio sources. Filled circles indicate positive RM s, open circles negative RM s. The area of the circles is proportional to $|RM|$ within limits of 5 and 150 rad/m^2 (from Han *et al.*, 1997).

RM s measured against extragalactic sources are more difficult to interpret because of the long sightlines and contamination from the sources. The results indicate that the magnetic field has a substantial **random component**, especially above the plane.

4. Zeeman Measurements at 21 cm

Proposed by Bolton & Wild:
ApJ 125 296 1957
(short Note In ApJ)

Useful detailed discussion:
Crutcher et al.
ApJ 407 175 2003

OH for molecular clouds,
e.g., Crutcher & Troland
ApJ 537 L139 2000

Review: Sec. 3 of Crutcher,
Heiles, & Troland, Springer
Lec. Notes in Physics,
614 155 2003

NOTES

ON THE POSSIBILITY OF MEASURING INTERSTELLAR MAGNETIC FIELDS BY 21-CM ZEEMAN SPLITTING

Measurement of the small magnetic field believed to exist in interstellar space has so far eluded both optical and radio techniques. However, the introduction of large radio reflectors offers the possibility of determining longitudinal fields in localized interstellar regions by observing the Zeeman splitting of the 21-cm line of neutral hydrogen.

In the presence of a weak magnetic field, the 21-cm line is split into three components, of frequency (Nide and Nelson 1948)

$$\begin{aligned} \nu_0 &= \nu_0 \\ \nu_0 \pm \frac{eH}{4\pi m c} &= \nu_0 \end{aligned} \quad (1)$$

where ν_0 is the unsplit frequency of the line and H the longitudinal component of the magnetic field. Numerically, the frequency difference, $\Delta\nu$, between the two π components is 2.8 Mc/s per gauss. Thus a magnetic field of 10^{-4} gauss, such as is believed to exist in the Galaxy, gives $\Delta\nu = 30$ c/s.

Under normal circumstances the detection of such small shifts in the galactic emission profiles would hardly be possible, owing to their large Doppler broadening. On the other hand, relatively narrow profiles have been observed in absorption. Hagen, Lilley, and McClain (1955) have reported three narrow absorption lines in the 21-cm spectrum of the discrete source in Cassiopeia, presumably due to three individual H I concentrations with different radial velocities. These lines have half-widths of about 10 kc/s, in the order of which the radiation is almost completely absorbed. It may reasonably be assumed that the magnetic field is sensibly constant in direction over any one of the H I concentrations responsible for the absorption lines.

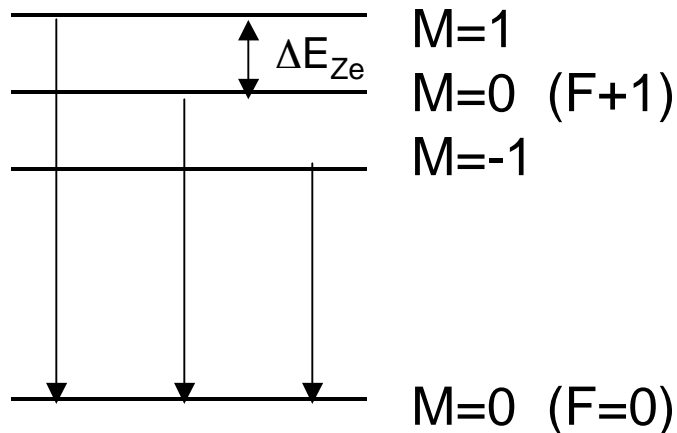
The detection of a Zeeman shift less than 1 per cent of the line width could be accomplished by using the radio analogue of the optical method currently employed by Radock (1951) for measuring weak solar fields. The frequency of a narrow-band receiver is set on the edge of the line near the point of maximum steepness, and the polarization of the antenna is switched to receive the two circular components alternately. The output at the switching frequency is given, in units of antenna temperature, by

$$\Delta T = \frac{T_a \Delta\nu}{\nu}$$

where T_a is the maximum decrease in antenna temperature of the absorption line, $\Delta\nu = 2.8 \times 10^6$ c/s is the difference in frequencies between the two π components, and ν is the half-width of the absorption line, assumed of gaussian profile. Current results indicate values of T_a of the order of 1000° K if the Cassiopeia absorption lines are observed with a 150-foot reflector. Hence, with $\nu = 10$ kc/s, we should expect $\Delta T = 3 \times 10^{-4}$ degrees. Current techniques permit the detection of $\Delta T = 1^\circ$ K (H = 3×10^{-4} gauss), and instrumental improvements on this figure are likely in the future.

Physical Basis for Using the Zeeman Effect

Zeeman splitting of the ground level of HI



F is the total angular momentum, electron plus nuclear. with the latter ignored here

For the magnetic fields of interest, the Zeeman splitting

$$E_Z = \frac{e\hbar}{2m_e c} B = 1.400 \text{ Hz} \left(\frac{B}{\mu\text{G}} \right)$$

is negligible compared to the basic hfs splitting (1420 MHz).

Observing along the field, there are two circular polarized (σ) components, $\Delta M = \pm 1$.

Perpendicular to the field, there are three plane polarized (π) components, $\Delta M=0, \pm 1$

Observing circularly polarized radiation measures $B_{||}$

Application of the 21-cm Zeeman Effect

If the 21-cm transition were not (thermally and turbulently) broadened, the polarization capability of radio receivers could resolve the Zeeman effect and measure the field directly.

If the field has a component along the line of sight, the broadened line wings will be circularly polarized, so Bolton and Wild suggested that the intensity difference between the line wings should be measured. This difference (Stokes parameter V) is related to the derivative of the unpolarized intensity I .

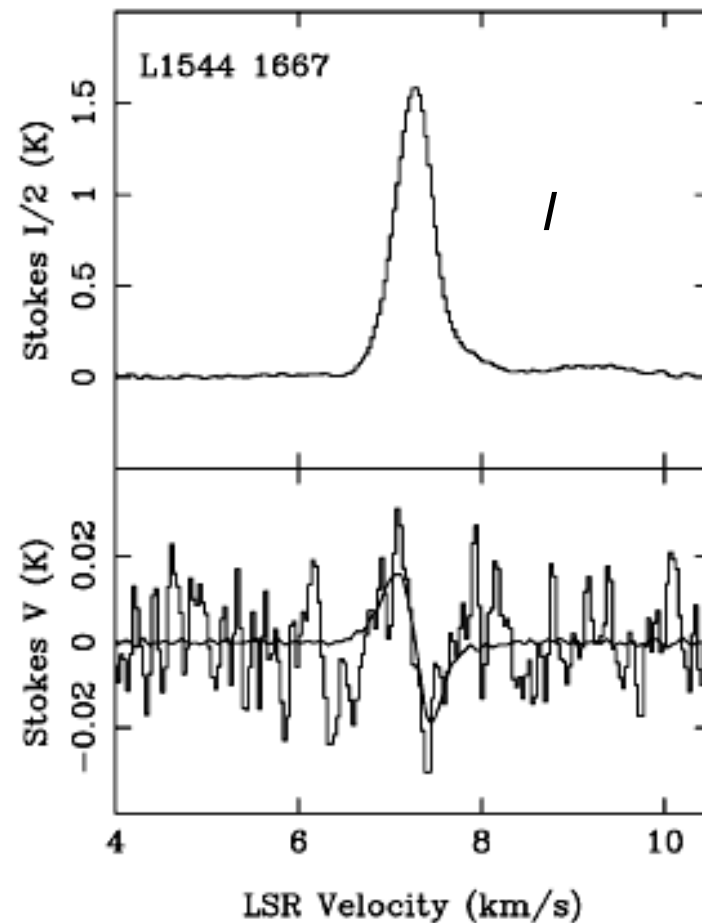
$$V = \frac{dI}{d\nu} \nu_{Zm} \cos \vartheta$$

where ν_{Zm} is the Zeeman frequency and θ is the angle between **B** and the line of sight.

Determining the Parallel Component of the Field from V and dI/dv

Example comparing the Stokes V spectrum with the derivative of the unpolarized intensity.

Crutcher & Troland
ApJ 537 L39 2000:
OH in the core of L1544



Addendum on the Stokes Parameters

From Rybicki & Lightman, an EM wave can be expressed using either the observer's x - y frame or the principle axes of a polarization ellipse. The angle β gives the components in the former, and χ is the angle that the principle axis makes with the x -axis.

$$E_x = \mathcal{E}_0(\cos \beta \cos \chi \cos \omega t + \sin \beta \sin \chi \sin \omega t)$$

$$E_y = \mathcal{E}_0(\cos \beta \sin \chi \cos \omega t - \sin \beta \cos \chi \sin \omega t)$$

The Stokes parameters are then defined as:

$$I \equiv \mathcal{E}_1^2 + \mathcal{E}_2^2 = \mathcal{E}_0^2$$

$$Q \equiv \mathcal{E}_1^2 - \mathcal{E}_2^2 = \mathcal{E}_0^2 \cos 2\beta \cos 2\chi$$

$$U \equiv 2\mathcal{E}_1 \mathcal{E}_2 \cos(\phi_1 - \phi_2) = \mathcal{E}_0^2 \cos 2\beta \sin 2\chi$$

$$V \equiv 2\mathcal{E}_1 \mathcal{E}_2 \sin(\phi_1 - \phi_2) = \mathcal{E}_0^2 \sin 2\beta.$$

Note that, in addition to the unpolarized intensity I , there are only two independent parameters (the direction of the polarization).

All this is mathematical: The problem is to express the results of a given polarization experiment in terms of these parameters.

For the radio Zeeman measurements, see Crutcher et al. (1993)

Results of 21-cm Zeeman Measurements

Preliminary results for the CNM
(Heiles, Crutcher, & Troland 2003)

There is a lot of scatter.
Non detections not shown.
Typical field is $B_{\parallel} = 5 \mu\text{G}$.

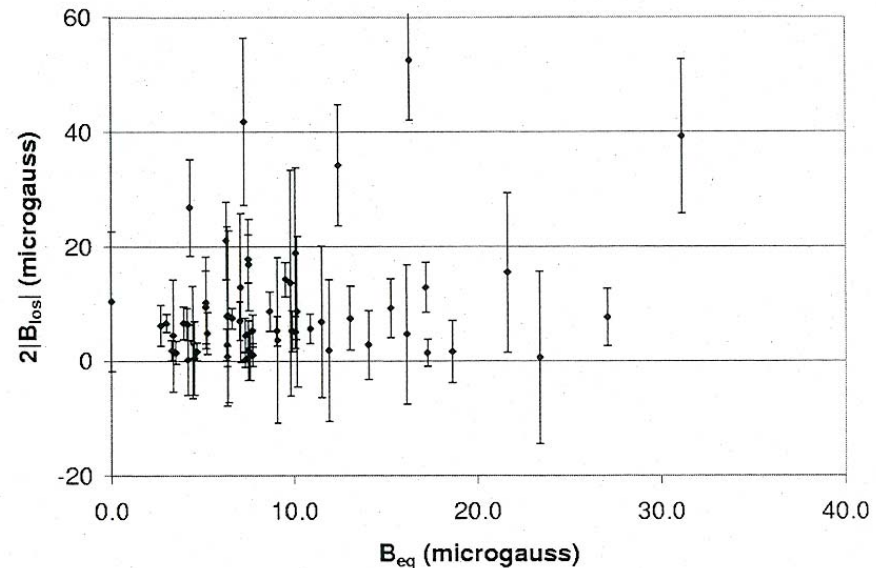
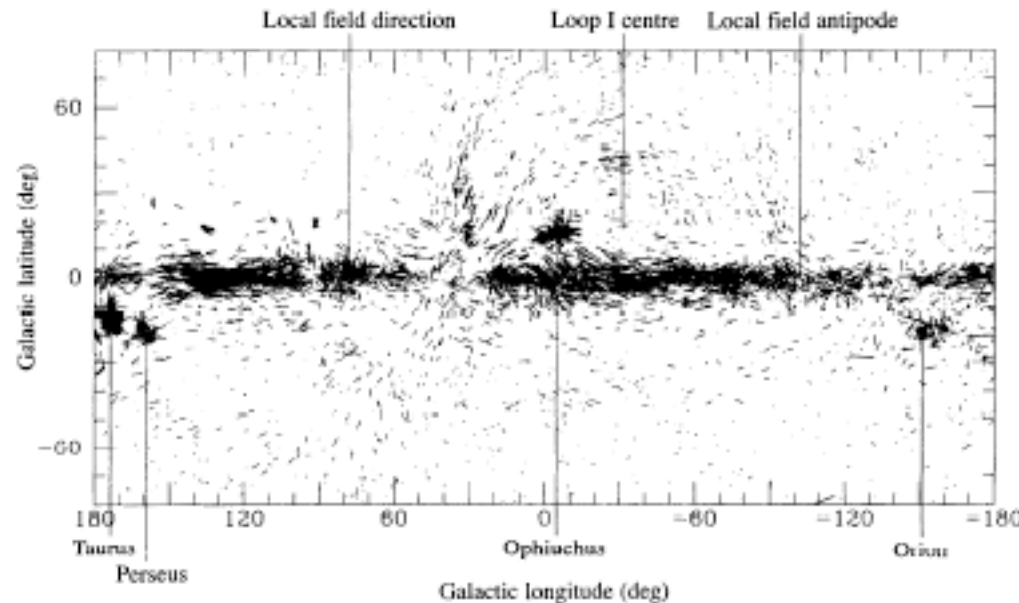


Fig. 2. Arecibo H I Zeeman results; here $B_{\text{los}} \equiv B_{\parallel}$

Final result of the Millenium Arecibo 21 cm Survey
Heiles & Troland, ApJ 624, 771, 2005
Median line of sight magnetic field: $6.1 \pm 1.8 \mu\text{G}$

Results for dark cloud & cores will be discussed later.

Starlight Polarization Map of the Galaxy



light lines:
polarization
< 0.6% with
extended lines

B_{\perp} for $\sim 10^4$ nearby stars, polarization (c.f. magnetic alignment of dust grains), yields directions of the plane in the sky magnetic field.
source: Zweibel & Heiles, Nature, 385, 131, 1997

- 1. The galactic field is “mainly in the plane”.***
- 2. It is strong along the local spiral arm.***
- 3. Random component is up to 50% larger than uniform.***
- 4. Out of plane features are associated with loops and regions of star formation.***

4. Summary

Different techniques measure different things, e.g., field components parallel (RM & Zeeman) and perpendicular (synchrotron and dust polarization). Zeeman measurements are sensitive to neutral regions, and synchrotron emission is particularly useful for external galaxies..

For the Milky Way, the field is mainly parallel to the disk midplane, concentrated in the spiral arms with inter-arm reversals, and twice as large as the older value of $3 \mu\text{G}$. The random component may be 50% of the ordered field. The median total field in the solar neighborhood is $6 \mu\text{G}$. The field increases with decreasing galactic radius, and is about $10 \mu\text{G}$ at $R = 3 \text{ kpc}$

Summary (concluded)

For external galaxies, the **synchrotron** emission studies show the effects of spiral structure, the existence of thin and thick disk components, and occasionally inter-arm reversals. Typical field values are $10 \mu\text{G}$, not all that different than the Milky Way.

For more on magnetic fields in external galaxies, see: R. Beck, SSR 99 243 2001.

Cosmic rays and magnetic fields both have important dynamical consequences for the ISM that will be discussed in Lecture 12.